

DENSITY FUNCTIONAL THEORY STUDY OF 5-PHENYL-1,3,4-OXADIAZOLE-2-THIOL AND ITS DERIVATIVES AS PHOTSENSITIZERS FOR DYE-SENSITIZED SOLAR CELLS

D. Sudha¹, V. Sathyanarayanamoorthi² and K. Uthayarani¹, ✉

¹Department of Physics, Sri Ramakrishna Engineering College, Coimbatore-641 022,
(Tamilnadu) India

²Department of Physics, PSG College of Arts and Science, Coimbatore-641 014,
(Tamilnadu) India

✉Corresponding Author: uthayarani.karunakaran@srec.ac.in

ABSTRACT

The cornerstone of the present study is the theoretical analysis of electronic and redox properties of 5-phenyl-1,3,4-oxadiazole-2-thiol dyes using DFT with B3LYP/6-311+G (d,p) level. In this investigation, the dye properties were carried out in both the gas and solvent phases. The ground and excited state oxidation potentials, as well as electron injection from the dyes to semiconductor TiO₂, are reported. The calculation shows that all of the dyes can potentially be good photosensitizers in DSSC. Their LUMOs lie over the E_{cb} of TiO₂ and their HOMOs lie under the reduction potential energy of the electrolytes corresponding to the ability of electron transfer from the dye excited state to TiO₂. The study of structural, electronics and optical properties for these compounds could help to design more efficient functional photovoltaic organic materials.

Keywords: 5-phenyl-1,3,4-oxadiazole-2-thiol, Organic dyes, Dye-sensitized Solar Cells, Light-harvesting Efficiency, Density Functional Theory.

RASAYAN J. Chem., Vol. 14, No.3, 2021

INTRODUCTION

Dye-sensitized solar cells (DSSCs) have been regarded as one of the most promising next-generation photovoltaic cells due to their potentially low fabrication costs, easy production, and flexibility compared to traditional silicon-based solar cells.¹ The sensitizer plays a significant role in improving the efficiency of DSSCs. Therefore, considerable synthetic works have been carried out on Ru-based sensitizers^{2,3} and metal-free organic dye sensitizers.⁴⁻⁹ The dye-sensitized solar cell (DSSC) uses molecules to absorb photons and separates the two functions of light-harvesting and charge-carrier transport. The advantage of this kind of solar cell is that it is compatible with various supporting materials and can be produced under mild conditions.¹⁰

The basic structure of most of the organic sensitizers is made of a donor (D), a bridge (B, typically a π spacer), and an acceptor (A) moiety, which are usually combined following D- π -A rod-like configuration to improve the efficiency of the UV/vis photoinduced intramolecular charge transfer (ICT). Generally, the critical factors that influence the sensitization are (i) the excited-state redox potential has to match the energy of the conduction band (CB) edge of the semiconductor; (ii) the highest occupied molecular orbital (HOMO) must fit redox potential, and the lowest unoccupied molecular orbital (LUMO) has to be higher in energy; (iii) a huge light-harvesting ability of the dye is crucial to get a substantial photocurrent response; (iv) the good conjugation across the donor and anchoring group determines the large charge transfer (CT) character of the electronic transition; (v) the electronic coupling strength between dye's LUMO and the semiconductor CB is, of course, a key property for efficient electron injection from the dye onto the semiconductor surface. Note that in general, the major factors leading to a low conversion efficiency of many organic dyes in DSSC are the formation of dye aggregates and charge recombination between the CB electrons and the dye or the electrolyte. To further design and develop more efficient metal-free dyes for DSSCs, appropriate DBA systems are needed whose properties can be finely tuned by applying adequate

structural modifications. Recently, it has been found that triphenylamine (TPA)-like moieties and a cyanoacetic acid group are units of choice as electron donor and electron acceptor/anchoring groups, respectively.¹¹⁻¹³ Indeed, the TPA moiety is expected to greatly confine the cationic charge from the semiconductor surface and efficiently hamper the recombination. TPA also shows a huge steric hindrance and can therefore prevent unfavorable dye aggregation at the semiconductor surface.¹⁴

The interest in organic sensitizing dyes for usage in DSSCs has been growing quickly over the past few years. All-organic dyes have shown promising potential as an effective sensitizer in dye-sensitized solar cells (DSSCs).¹⁵ The design concept of all-organic dyes to improve light-to-electric-energy conversion is discussed based on absorption, electron injection, dye regeneration, and recombination. In DSSCs, the photosensitizer is one of the most important components influencing solar cell performance, because the choice of sensitizer determines the photoresponse of the DSSC and initiates the first steps of photon absorption and therefore the subsequent electron transfer process. In addition to standard Ru-complex sensitizers, metal-free analogs within the sort of organic dyes have also been investigated in DSSCs. The photovoltaic performance of organic dye sensitizers has continually improved.¹⁶

To achieve higher performances for solar cells based on organic dyes, comparable to those for solar cells based on Ruthenium complexes, sophisticated molecular design of organic dyes is required. For this purpose, 5-Phenyl-1,3,4-Oxadiazole-2-thiol dye and its derivatives were selected to improve both solar cell performance and the long-term stability of the solar cells. Based on the detailed molecular design of 5-Phenyl-1,3,4-Oxadiazole-2-thiol dye and their derivatives, the photovoltaic performance was reported.

EXPERIMENTAL

Computational Methods

Two powerful methodologies namely ab initio and density functional theory (DFT) have been developed to compute solutions for the many-electron systems. DFT/Time-dependent DFT (TDDFT) is the most often used theoretical approach to investigate the ground state and excited state properties of photo-sensitizer. DFT is the method of choice for large systems and even for molecular dynamics calculations. It is more computationally efficient than the Hartree-Fock methods.¹⁷ The accuracy of DFT is based on approximations and so-called exchange-correlation functional and it is computed through various models and approximate methods.

In the present work, 5-Phenyl-1,3,4-oxadiazole-2-thiol dye molecule and newly designed dyes were performed to determine geometrical electronic structure and spectra using Density Functional theory. All the calculations were performed both in the gas and solvent phase using Gaussian 09 package.¹⁸ The basis set B3LYP function and 6-311+G(d,p) has been used. The polarizable Continuum Model (PCM) has been used for the study of solvent effects.

This section, it is focused on the evaluation of the electrochemical properties of the dyes in their excited states. The free energy change for electron injection onto a titanium dioxide surface is:

$$\Delta G^{inject} = E_{ox}^{dye*} - E_{CB}^{TiO_2} \quad (1)$$

Where, E_{ox}^{dye*} is the oxidation potential of the dye in the excited state, and $E_{CB}^{TiO_2}$ is the energy of the conduction band of the TiO_2 (-4.0eV) semiconductor.¹⁹ The model used for the evaluation of E_{ox}^{dye*} implies that the electron injection occurs from the unrelaxed excited state. For this reaction path, the excited-state oxidation potential can be extracted from the redox potential of the ground state E_{ox}^{dye} , and the absorption energy associated with the photo-induced ICT (λ_{max}^{ICT}) according to:

$$E_{ox}^{dye*} = E_{ox}^{dye} - \lambda_{max}^{ICT} \quad (2)$$

Where, λ_{max}^{ICT} is the energy of the intermolecular charge transfer.

The efficiency of DSSC is the performance of the dyes in responsibility to the incident light. Based on the light-harvesting efficiency of the dyes, the value has to be as high as possible to maximize the photocurrent response. The light-harvesting efficiency (LHE) was determined by formula.²⁰

$$LHE = 1 - 10^{-f} \quad (3)$$

Where f is the Oscillator's strength of the dye.

RESULTS AND DISCUSSION

A systematic comparison of frontier molecular orbitals and absorption spectra of 5-phenyl-1, 3, 4-oxadiazole-2-thiol, and newly designed dyes are carried out. Furthermore, the light-harvesting efficiency (LHE) and the driving force of electron injection (ΔG_{inject}) are calculated. In addition, the electron coupling of 5-phenyl-1,3,4-oxadiazole-2-thiol is simulated by the DFT method to testify the electron injection efficiency. This work is expected to reveal the effect of chemical modification on the DSSCs efficiency and provide valuable guidance for developing efficiency dyes.²¹⁻²⁹

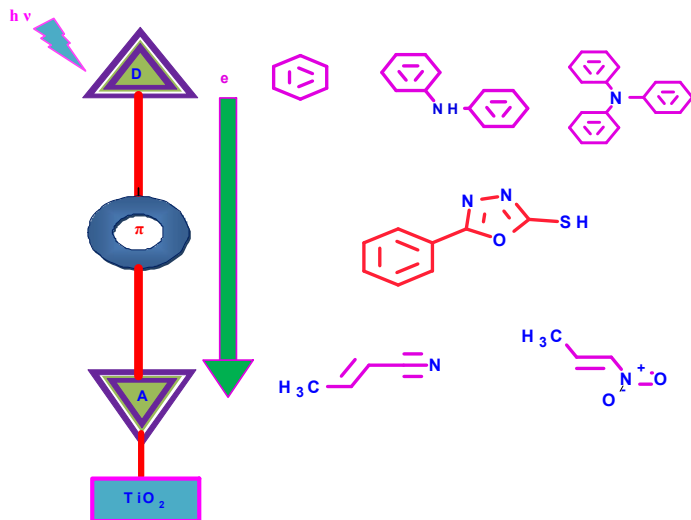


Fig.-1: Different Parts of D- π -A system, D = Donor, π = pi-spacer, A = Acceptor

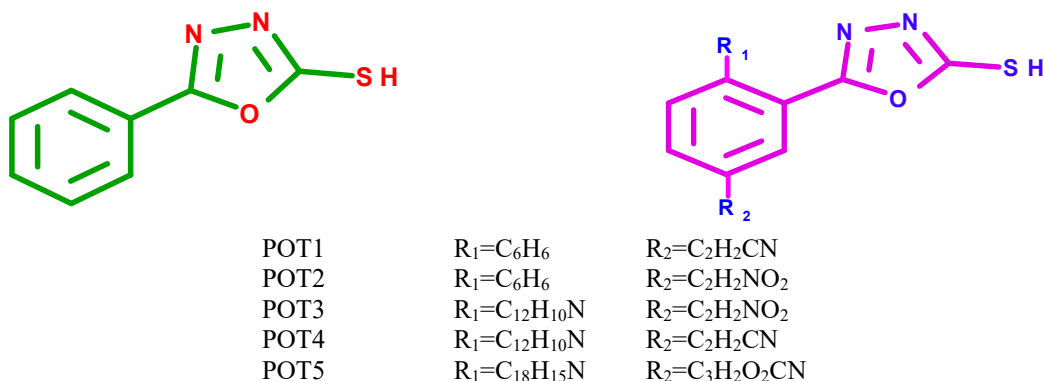
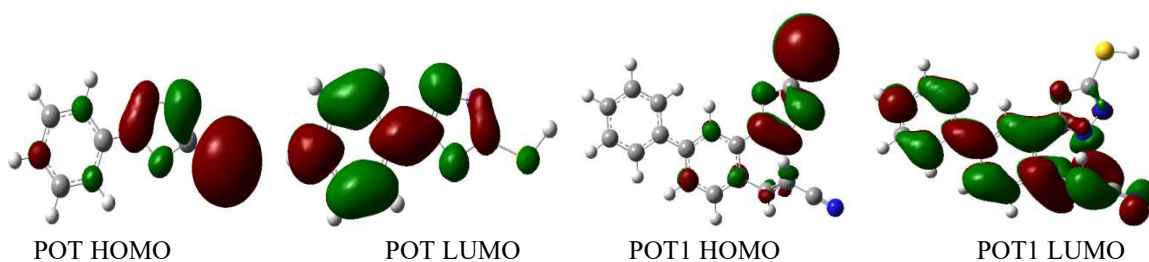


Fig.-2: Chemical Structure of 5-phenyl-1,3,4-oxadiazole-2-thiol [POT] and Newly Designed Dyes

Electronic Structure

The ground-state structure for 5-Phenyl-1,3,4 -oxadiazole- 2- thiol and newly designed dyes were carried out at the B3LYP level. The discussion based on geometrical parameters of the ground state structure is neglected. The distribution patterns of highest occupied molecular orbitals (HOMO) and lowest unoccupied molecular orbitals (LUMO) are used to study the efficiency of sensitizers and they are shown in Fig.-3 and 4 in Table-1, we have tabulated the computed HOMOs energies, LUMOs energies, and energy gap of the POT-based sensitizers at B3LYP/6-311+G(d,p) level theory.



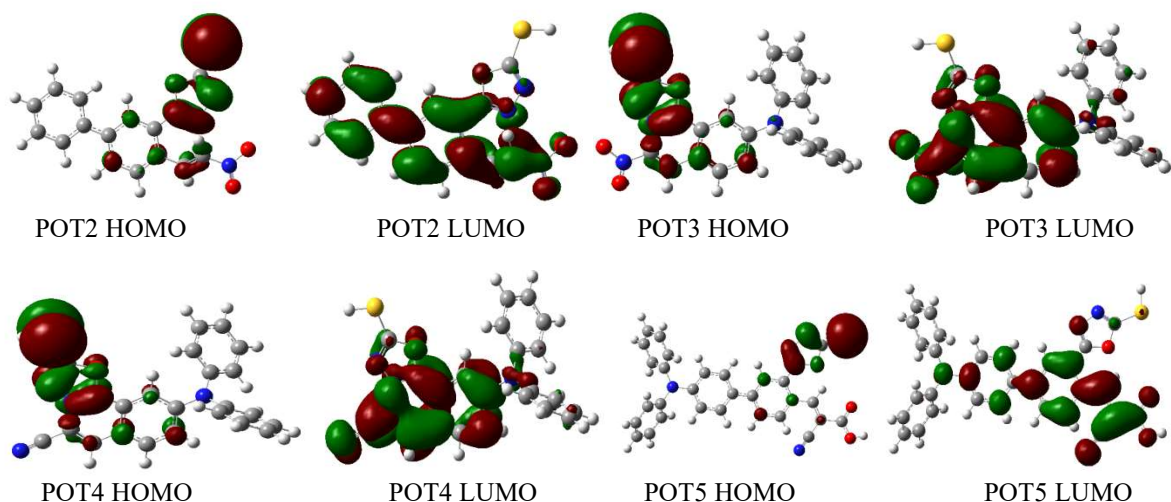


Fig.-3: The HOMO and LUMO Distribution Pattern of Dyes at DFT / B3LYP/6-311+G* Level of Theory in Gas Phase

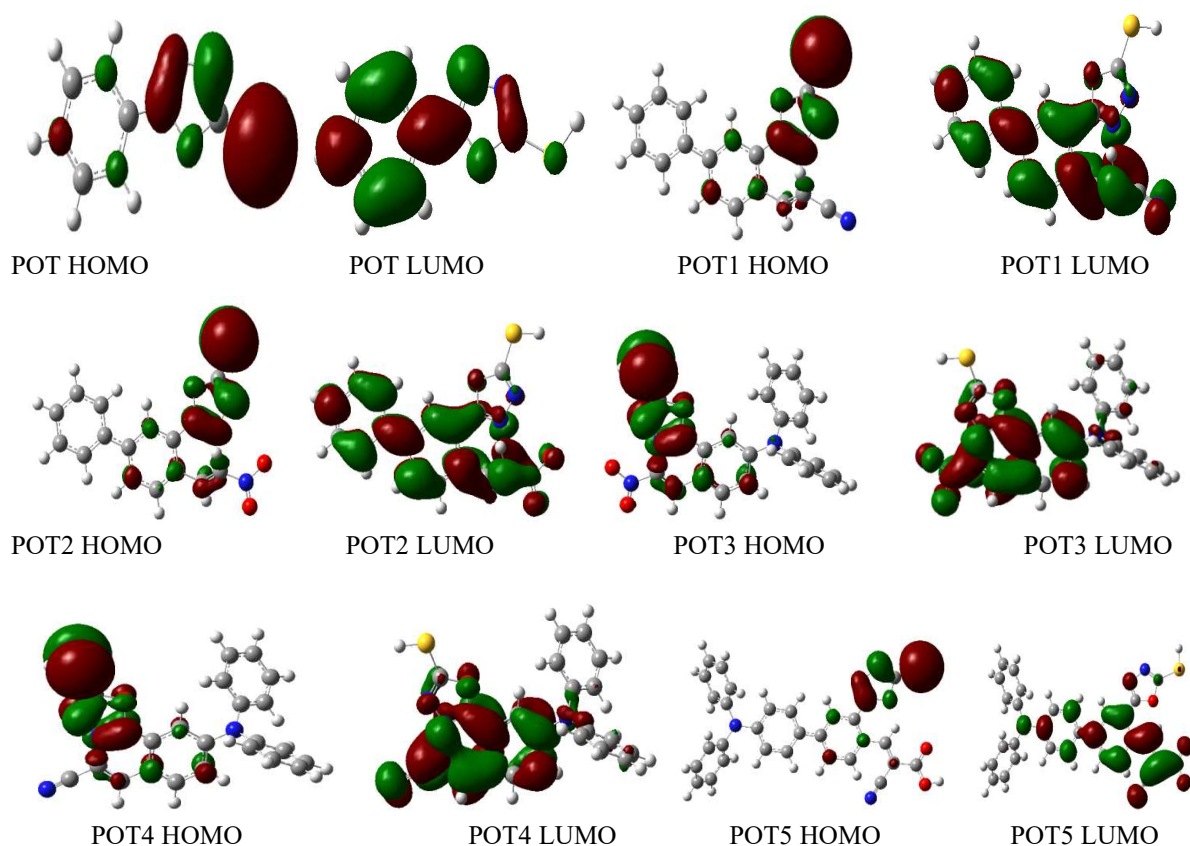


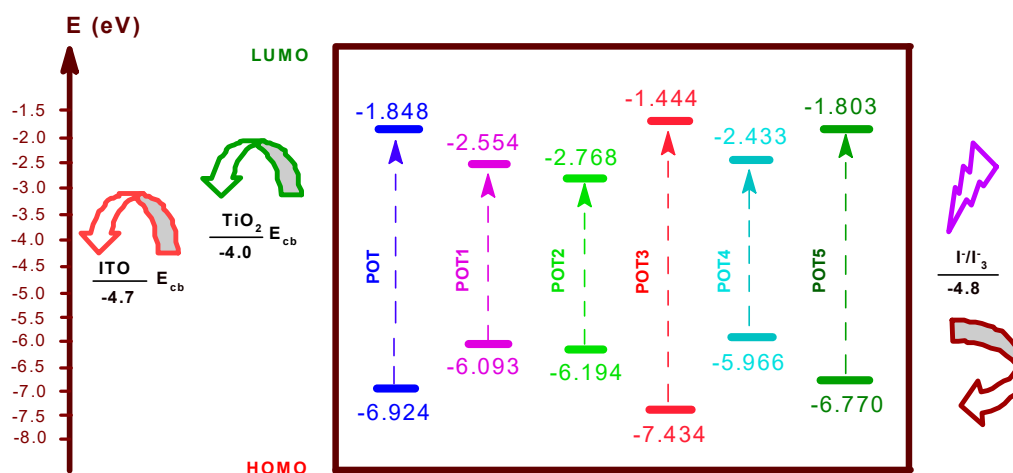
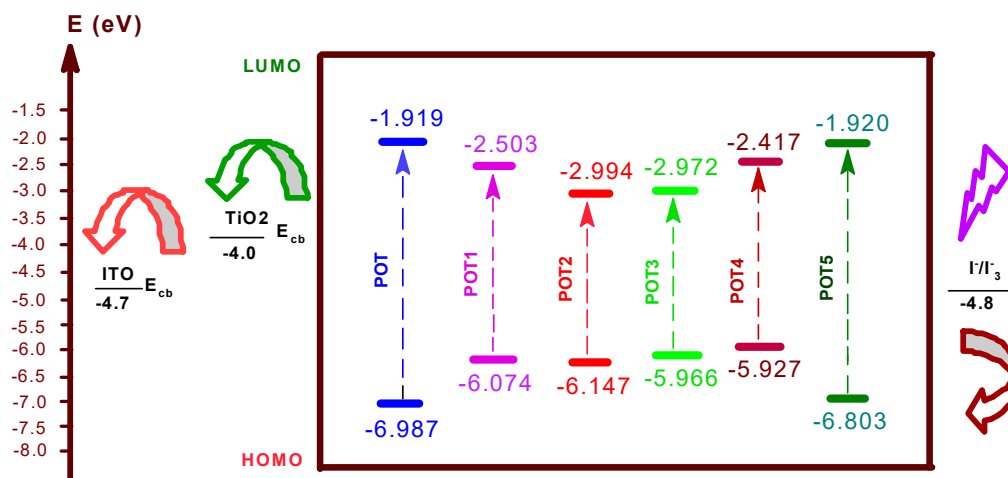
Fig.-4: The HOMO and LUMO Distribution Pattern of Dyes at DFT / B3LYP/6-311+G* Level of Theory in PCM

The trend of HOMO energies is POT4> POT1> POT5> POT> POT3 in gas phase and POT4> POT3> POT1> POT2> POT5> POT in solvent medium. Whereas LUMO energies is POT3> POT5> POT> POT4> POT1> POT2 in gas phase and POT> POT5> POT4> POT1> POT3> POT2 in solvent medium. It can also be observed that elongating the bridge E_g usually decreases. The smaller energy gap of POT1, POT2 and POT4 than POT, POT3 and POT5, so those DSSCs performances of the sensitizers have been greater than the later one. In the case of solvent medium POT1, POT2, POT3 and POT4 provide better performance.

Table-1: The E_{HOMO} , E_{LUMO} and Energy Gap (E_g) of Dyes in eV at B3LYP/6-311+G Level of Theory

System	Gas Phase			DMF		
	E_{HOMO}	E_{LUMO}	E_{gap}	E_{HOMO}	E_{LUMO}	E_{gap}
POT	-6.9239	-1.8484	5.0755	-6.9871	-1.9192	5.0678
POT1	-6.0929	-2.5540	3.5388	-6.0739	-2.5031	3.5707
POT2	-6.1944	-2.7685	3.4259	-5.9664	-2.9940	3.1524
POT3	-7.4336	-1.4438	5.9898	-5.9664	-2.9715	2.9949
POT4	-5.9661	-2.4329	3.5331	-5.9269	-2.4169	3.5100
POT5	-6.7703	-1.8028	4.9675	-6.8026	-1.9200	4.8825

Considerably lowered LUMO energy levels would not only enhance the electron injection ability but also make such sensitizers unsusceptible to oxidation. The smaller E_{LUMO} of POT3 and POT5 sensitizers also showed that inject electrons might be supplementarily tabulated, which would result in hindering the quenching. However, the most positive value of the energy gap is found in POT3 in the gas phase. The least value of the energy gap is found in the same dye in a solvent medium. The significance of redshift has been observed in the case of di-phenyl and tri-phenyl substituted sensitizers which revealed that it is efficient visible light sensing or absorbing sensitizers. Moreover, it is also expected that these dyes can be used as sensors having the sensing aptitudes of metal ions in the UV-vis wavelength. The energy level diagram of the HOMO and LUMO of the dyes, E_{cb} of TiO_2 and redox potential energy of the electrolyte, are presented in Fig.-5 and 6.

Fig.-5: Schematic Energy Diagram of Dyes, TiO_2 and Electrolyte (I^-/I_3^-). E_{HOMO} and E_{LUMO} of the Dyes are in Gas PhaseFig.-6: Schematic Energy Diagram of Dyes, TiO_2 and Electrolyte (I^-/I_3^-). E_{HOMO} and E_{LUMO} of the Dyes are in DMF

λ_{\max} , ΔG_{inject} , E_{ox}^{dye} , E_{ox}^{dye*} , λ_{\max}^{ICT} are given in Table-2. In investigated derivatives then $|V_{RP}|$ and ΔG_{inject} is superior as compared to the POT. The $|V_{RP}|$ and ΔG_{inject} for POTs has been observed as 0.876 and -1.753 in the gas phase and 0.795 and -1.791 in DMF respectively. By comparing those values with newly designed dyes, it has been found that the newly designed dyes would be efficient sensitizers. The derivatives containing CN have superior LHE as compared to other systems. Based on the electron activating group, the trend to enhance LHE has been observed as $\text{CN} > \text{NO}_2$. We observed that systems having COOH as substituent has higher ΔG_{inject} and $|V_{RP}|$ as compared to the derivatives containing NO_2 .

UV-Vis Absorption Spectra

An efficient photosensitizer exhibits intense absorption in the visible region (400 nm to 700 nm).³⁰ The transition (HOMO to LUMO level) characters in the (DMF) solvent and gas phase are different. The oscillator strength also increases in the solvent phase differs from that of the gas phase in the studied molecules. The decrease in absorption wavelength in the solvent phase is due to the addition of polar solvent.³¹

The simulated absorption spectra of the six POT dyes in the gas phase and solvent medium are shown in Fig.-7 and 8. The first optically allowed electronic transitions of POT, POT1, POT2, POT3, POT4, and POT5 are predicted to populate the HOMO→LUMO transitions at 265.09, 435.35, 453.18, 385.18, 436.72 and 390.25 in the gas phase and 270.85, 427.53, 493.45, 504.97, 434.42 and 406.46 nm respectively for solvent medium. It seems that the calculated result reproduces the considerable redshift of the spectra in the solvent phase. Therefore, the inclusion of the solvent is important to calculate the spectra for considerable redshift.

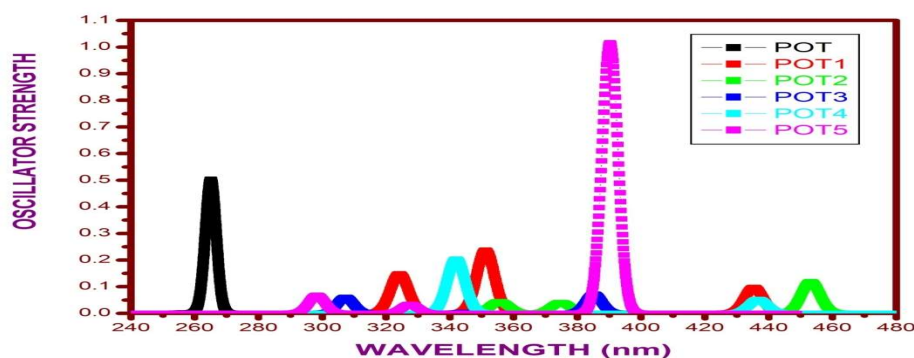


Fig.-7: Simulated Absorption Spectra of Dyes calculated in Gas Phase at TDDFT / B3LYP/6-311+G(d,p) Level of Theory

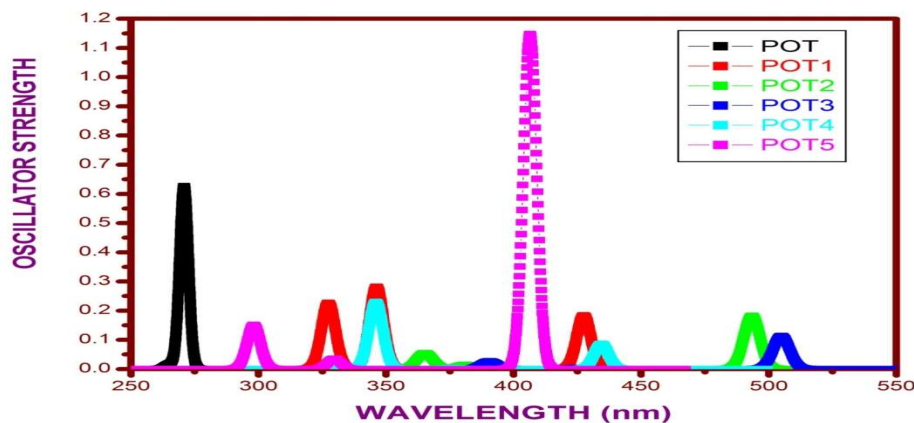


Fig.-8: Simulated Absorption Spectra of Dyes calculated in DMF at TDDFT / B3LYP/6-311+G(d,p) Level of Theory

The structural modifications improving the electron injection efficiency of the POT-based DSSCs. Of course, all modifications are theoretically possible and a large panel of new structures can be tested. Therefore, we impose that all dyes possess terminal of either C_2H_4N or $C_2H_4NO_2$ group on the acceptor unit is necessary to link the dye to the semiconductor surface. In this work, it has been focused on and the free energy of injection (ΔG_{inject}), the oxidation potential of the dye must be positive, and the light-harvesting efficiency of the dye to be as high as possible to maximize the photocurrent response. The comprehensive intramolecular charge transfer has been observed from the donor to the acceptor side. The diphenyl and triphenyl substitution in the donor site are favorable to enhance (ΔG_{inject}) and $|V_{RP}|$.

Table-2: Calculated absorption spectra λ_{max} nm, ΔG^{inject} , oxidation potential, intramolecular charge transfer energy of dyes at B3LYP/6-311+G level of energy

System	Gas Phase					DMF				
	λ_{max}	ΔG^{inject}	E_{ox}^{dye*}	E_{ox}^{dye}	λ_{max}^{ICT}	λ_{max}	ΔG^{inject}	E_{ox}^{dye*}	E_{ox}^{dye}	λ_{max}^{ICT}
POT	265.09	-1.753	2.247	6.924	4.677	270.85	-1.591	2.409	6.987	4.578
POT1	435.35	-0.754	3.246	6.093	2.847	427.53	-0.827	3.173	6.073	2.900
POT2	453.18	-0.541	3.459	6.194	2.735	493.45	-0.367	3.633	6.146	2.513
POT3	385.18	0.215	4.215	7.434	3.219	504.97	-0.480	3.511	5.966	2.455
POT4	436.72	-0.873	3.127	5.966	2.839	434.42	-0.928	3.072	5.926	2.854
POT5	390.25	-0.407	3.593	6.770	3.177	406.46	-0.254	3.746	6.802	3.050

Light-Harvesting Efficiency (LHE) and Oscillator Strength

The light-harvesting efficiency (LHE) is the efficiency of the dye to respond to the light. It is another factor that indicates the efficiency of DSSC. The light-harvesting efficiency (LHE) of the dye should be as high as possible to increase the photocurrent response. The LHE of all the dyes is calculated and listed in Table-3. The LHE of all the dyes in the gas phase is in the range of 0.057 to 0.489 and in the DMF, they are in the range of 0.118 to 0.504. The LHE values for the dyes are in a narrow range. As a result of Light-harvesting efficiency, the POT5 has been observed to be 0.489 and 0.503 in the gas phase and solvent medium respectively. Thus, it has been concluded that the introduction of amine derivatives in the donor side enhances the LHE and it is nicely comparable with the earlier studies. These dyes will convert more light into electricity.

Table-3: Excitation energy (E), Light Harvesting Efficiency (LHE) and Average Light Harvesting Efficiency ($LHE_{Average}$) of dyes at B3LYP/6-311+G level of theory

System	Gas Phase				DMF			
	E (eV)	λ (nm)	LHE	LHE_{avg}	E (eV)	λ (nm)	LHE	LHE_{avg}
POT	4.6771	265.09	0.683	0.352	4.5777	270.85	0.764	0.401
	4.7155	262.93	0.021		4.6792	264.97	0.037	
POT1	2.8479	435.35	0.201	0.311	2.9000	427.53	0.345	0.411
	3.5301	351.22	0.421		3.5802	346.30	0.477	
POT2	2.7359	453.18	0.239	0.163	2.5126	493.45	0.343	0.187
	3.3076	374.85	0.088		3.2526	381.19	0.032	
POT3	3.2189	385.18	0.153	0.080	2.4553	421.97	0.229	0.118
	3.5878	345.57	0.008		2.9174	335.73	0.008	
POT4	2.8390	436.72	0.113	0.057	2.8540	434.42	0.179	0.209
	3.2770	378.35	0.001		3.3008	375.62	0.007	
POT5	3.1771	390.25	0.904	0.489	3.0503	406.46	0.929	0.504
	3.7854	327.53	0.074		3.7605	329.70	0.078	

The oscillator strength is directly obtained from DFT calculation. The POT dye has two main absorption peaks (265 and 390 nm in the gas phase, 270 and 406 nm in solvent phase DMF). The oscillator strength and transition character are given in Table-4. Only the transition with considerable oscillator strengths is given. The electron structure of the four newly designed sensitizers is quite similar to one another even though their substituent is different.

Table-4: Oscillator strength (f) and Transition character of dyes (H=HOMO L=LUMO, L+1=LUMO+1, etc) at B3LYP/6-311+G level of theory

System	Gas Phase			DMF		
	λ (nm)	f	Transition character	λ (nm)	f	Transition character
POT	265.09	0.4991	H \rightarrow L (100%)	270.85	0.6268	H \rightarrow L (100%)
	262.93	0.0091	H-1 \rightarrow L (90.6%)	264.97	0.0164	H-1 \rightarrow L (91.8%)
	257.21	0.0016	H \rightarrow L+1 (89.01%)	246.50	0.0007	H \rightarrow L+1 (85.4%)
POT1	435.35	0.0973	H \rightarrow L (100%)	427.53	0.1839	H \rightarrow L (100%)
	351.22	0.2370	H \rightarrow L+1 (86.8%)	346.30	0.2818	H \rightarrow L+1 (85.1%)
	324.21	0.1483	H-1 \rightarrow L (79.5%)	327.42	0.2268	H-1 \rightarrow L (80.2%)
POT2	453.18	0.1189	H \rightarrow L (100%)	493.45	0.1823	H \rightarrow L (100%)
	374.85	0.0404	H \rightarrow L+1 (84.5%)	381.19	0.0140	H \rightarrow L+1 (79.3%)
	355.61	0.0439	H-1 \rightarrow L (80%)	365.22	0.0543	H-1 \rightarrow L (78.8%)
POT3	385.27	0.0722	H \rightarrow L (100%)	504.97	0.1134	H \rightarrow L (100%)
	345.57	0.0036	H-1 \rightarrow L (78.3%)	424.98	0.0038	H \rightarrow L+1 (81.11%)
	307.28	0.0600	H-1 \rightarrow L+1 (66.5%)	390.55	0.0265	H-1 \rightarrow L (78.85%)
POT4	436.72	0.0521	H \rightarrow L (100%)	434.42	0.0861	H \rightarrow L (100%)
	378.35	0.0006	H-1 \rightarrow L (87.6%)	375.62	0.0029	H-1 \rightarrow L (86.1%)
	342.00	0.2038	H-1 \rightarrow L+1 (82.6%)	346.06	0.2298	H-1 \rightarrow L+1 (82.3%)
POT5	390.25	1.0161	H \rightarrow L (100%)	406.46	1.1480	H \rightarrow L (100%)
	327.53	0.0334	H \rightarrow L+1 (81.6.1%)	329.70	0.0353	H \rightarrow L+1 (81.1%)
	298.35	0.0676	H-1 \rightarrow L (79.1%)	298.18	0.1510	H-1 \rightarrow L (78.9%)

Transition Character

Based on the analysis of the electron density of HOMO and LUMO, all the absorption behaviors of the dyes can be ascribed to the intramolecular charge transfer (ICT) character. The maximum absorption peak of POT and POT1 is located at 265.09 and 435.35 nm, respectively, which is contributed by the HOMO \rightarrow LUMO transition. The HOMO-1 of POT and POT1 is located at 262.93 and 324.21 nm respectively. Thus, it is reasonable to assign the 262.93 and 324.21 nm for POT and POT1 ICT characters. Similarly, the HOMO-1 of POT2 and POT3 is located at 355.61 and 345.57 nm respectively, and the HOMO-1 of POT4 and POT5 is located at 378.35 and 321 nm respectively. From the above calculations, it can be seen that all the absorption peaks of POT to POT5 are covering the entire visible region, which makes these dyes suitable for the application of DSSC.

Table-5: The electron injection (ΔG^{inject}), relative electron injection (ΔG_r^{inject}), oxidation potentials, light harvesting efficiencies (LHE), electron coupling constants ($|V_{RP}|$), absorption (λ_{max}) in nm, oscillator strengths (f) and transitions of POT dyes.

System	ΔG^{inject}	E_{ox}^{dye}	E_{ox}^{dye*}	λ_{max}^{ICT}	f	LHE	ΔG_r^{inject}	λ_{max}	$ V_{RP} $
POT	-1.591	6.987	2.409	4.578	0.627	0.764	1.000	270.85	0.796
POT1	-0.827	6.073	3.173	2.900	0.184	0.345	0.520	427.53	0.413
POT2	-0.367	6.146	3.633	2.513	0.182	0.343	0.231	493.45	0.183
POT3	-0.480	5.966	3.511	2.455	0.113	0.229	0.302	504.97	0.240
POT4	-0.928	5.926	3.072	2.854	0.086	0.179	0.583	434.42	0.464
POT5	-0.254	6.802	3.746	3.050	1.148	0.929	0.160	406.46	0.127

CONCLUSION

The UV-Visible spectroscopic properties, as well as the free energy of injection of systems POT– POT5, show that these dyes are the potential to be a good photosensitizer in DSSC. According to thermodynamic the spontaneous charge transfer process from the dye in an excited state to the conduction band of metal oxide need the LUMO energy of the dye to be more positive potential than the conduction band energy of metal oxide while the HOMO energy of the dye must be negative than reduction potential energy of the electrolyte. The superior electron injection and electron coupling constants of investigated systems are revealing that these derivatives show better DSSC properties. It can also be observed that by elongating the

bridge, the HOMO and LUMO energy gap decreases in 5-phenyl-1,3,4-oxadiazole 2-thiol. By using this theoretical procedure to gain insights into the geometrical and electronic structures of the dyes and bring out the adequate structural modification that will optimize the properties of the 5-phenyl-1,3,4-oxadiazole 2-thiol based dye-sensitized solar cells. Therefore, it can be concluded that further chemical modification of the dye such as adding high effective anchoring groups, bridges, or electron donor groups could raise the electron injection and light-harvesting efficiency of the DSSC with these photosensitizers.

REFERENCES

1. B. O' Reagen and M. Gratzel, *Nature*, **353**, 737(1991), <https://doi.org/10.1038/353737a0>
2. A. Goetzeger and C. Hebling, *Solar Energy Materials and Solar Cells*, **62**, 1(2000), [https://doi.org/10.1016/S0927-0248\(99\)00131-2](https://doi.org/10.1016/S0927-0248(99)00131-2)
3. A. Hagfeldt, M. Graetzel, *Chemical Reviews*, **95** (1), 49(1995), <https://doi.org/10.1021/cr00033a003>
4. M. Graetzel, *Nature*, **414** (6861), 338(2001), <https://doi.org/10.1038/35104607>
5. T.A. Heimer, E.J. Heilweil, C.A. Bignozzi, G.j. Meyer, *The Journal of Physical Chemistry A*, **104** 4256(2000), <https://doi.org/10.1021/jp993438y>
6. Nazeeruddin, M.K. Michael graetzel festschrift, *Coordination Chemistry Reviews*, **248**, 1161(2004).
7. P.V. Kamat, M. Haria, S. Hotchandani, *The Journal of Physical Chemistry B*, **108**, 5166(2004), <https://doi.org/10.1021/jp0496699>
8. J. Bisquert, D. Cahen, G. Hodes, S. Ruehle, A. Zaban, *The Journal of Physical Chemistry B*, **108** (24), 8106(2004), <https://doi.org/10.1021/jp0359283>
9. A. Furube, R. Katoh, T.Yoshihara, K. Hara, S. Murata, H. Arakawa, M. Tachiya, *The Journal of Physical Chemistry B*, **108**, 12583(2004), <https://doi.org/10.1021/jp0487713>
10. A. Mishra, M.k. Fischer, P. Bayerle, *Angewandte Chemie International Edition*, **48**(14), 2474(2009), <https://doi.org/10.1002/anie.200804709>
11. D. Liu, R.W. Fessenden, G.L. Hug, and P.V. Kamat, *The Journal of Physical Chemistry B*, **101**(14), 2583(1997), <https://doi.org/10.1021/jp962695p>
12. B. Burfeindt, T. Hannappel, W. Storck, and F. Willig, *The Journal of Physical Chemistry*, **100**(41), 16463(1996), <https://doi.org/10.1021/jp9622905>
13. K. Sayama, S. Tsukagochi, K. Hara, Y. Ohga, A. Shinpou, Y. Abe, S. Suga, H. Arakawa, *The Journal of Physical Chemistry B*, **106**, 1363(2002), <https://doi.org/10.1021/jp0129380>
14. Z. Ning , Q. Zhang, W. Wu , H. Pei , B. Liu, H. Tian, *Journal of Organic Chemistry*, **73**(10), 3791(2008), <https://doi.org/10.1021/jo800159t>
15. Sandra M. Feldt, Elizabeth A. Gibson, Erik Gabrielsson, Licheng Sun, Gerrit Boschloo and Anders Hagfeldt, *Journal of the American Chemical Society*, **132**(46), 16714(2010), <https://doi.org/10.1021/ja1088869>
16. T.Horiuchi, H. Miura, K. Sumioka, S.J. Uchida, *Journal of the American Chemical Society*, **126**, 39, 12218(2004), <https://doi.org/10.1021/ja0488277>
17. A.Furube, R.Katoh, T. Yoshihara, K. Hara, S.Murata, H.Arakawa, M.Tachiya, *The Journal of Physical Chemistry B.*, **108**,12588(2004), <https://doi.org/10.1021/jp0487713>
18. M. Frisch, J. et al. Gaussian 09, Revision A.1. Gaussian Inc, Wallingford, CT, 2009.
19. R. Katoh, A. Furube, T. Yoshihara, K. Hara, G. Fujihashi, S. Takano, S. Murata, H. Arakawa, M. Tachiya, *The Journal of Physical Chemistry B*, **108**, 4818(2004), <https://doi.org/10.1021/jp031260g>
20. Nalwa, H. S. Handbook of Advanced Electronic and Photonic Materials and Devices; Academic: San Diego, 2001.
21. M. Liang and J. Chen, *Chemical Society Reviews*, **42**(8), 3453(2013), <https://doi.org/10.1039/C3CS35372A>
22. W. Xu, B. Peng, J. Chen, M. Liang, and F. Cai, *Journal of Physical Chemistry C*, **112**(3), 874(2008), <https://doi.org/10.1021/jp076992d>
23. M. Liang, W. Xu, F. Cai et al., *Journal of Physical Chemistry C*, **111**(11), 4465(2007), <https://doi.org/10.1021/jp067930a>
24. H.-Q. Xia, J. Wang, F.-Q. Bai, and H.-X. Zhang, *Dyes and Pigments*, **113**, 87(2015), <https://doi.org/10.1016/j.dyepig.2014.07.033>

25. Muhammad Ramzan Saeed Ashraf Janjua, *Journal of the Chilean Chemical Society*, **63**, 1 (2018), <https://doi.org/10.4067/s0717-97072018000103850>
26. Imelda, Emriadi, Aziz H, Santoni. A, Utami. N, *Rasayan Journal of Chemistry*, **13(1)**, 121(2020), <https://doi.org/10.31788/RJC.2019.1245449>
27. Chundan Lin, Yanbing Liu, Di Shao, Guochen Wang, Huiying Xu, Changjin Shao, Wansong Zhang and Zhenqing Yang, *RSC Advances*, **11**, 3071(2021), <https://doi.org/10.1039/D0RA08815C>
28. Kadali Chaitanya, Xue-Hai Ju and B. Mark Heron, *RSC Advances*, **5**, 3978(2015), <https://doi.org/10.1039/C4RA09914A>
29. Kadali Chaitanya, Xue-Hai Ju and B. Mark Heronb, *RSC Advances*, **4**, 26621(2014), <https://doi.org/10.1039/C4RA02473G>
30. Umer Mehmood, Ibnelwaleed, A. Hussein, Khalil Harrabi and Shakeel Ahmed, *Advances in Materials Science and Engineering*, 286730, (2015), <https://doi.org/10.1155/2015/286730>
31. Juma Mzume Juma, Said Ali H. Vuai, N. Surendra Babu, *International Journal of Photoenergy*, 4616198, (2019), <https://doi.org/10.1155/2019/4616198>

[RJC-6501/2021]